An investigation on dry sliding wear behavior of Al6061/ Titanium carbide/ Basalt hybrid metal matrix composites

P. MUTHU*,[a]

*Corresponding author
Mechanical Engineering Department, University College of Engineering,
Anna University,
Ramanathapuram-623 513, Tamilnadu, India,
vpmuthu2001@yahoo.com

DOI: 10.13111/2066-8201.2021.13.4.12

Received: 26 February 2021/ Accepted: 01 October 2021/ Published: December 2021

Abstract: *Dry sliding wear plays an important role in selecting material for automotive and aerospace applications. Researchers have been exploring novel aluminum matrix composites (AMC), which offer minimum wear rate for various tribological applications. The present work involves multi-objective optimization for dry sliding wear behavior of Al6061 reinforced with 6 % of Titanium carbide and 4% of basalt hybrid metal matrix composites using principal component analysis (PCA)-based grey relational analysis (GRA). In this article, the effects of input variables of wear parameters such as applied load, sliding speed and sliding distance were investigated on different output responses, namely the wear rate, friction force and specific wear rate. Taguchi's L9 orthogonal array with three-level settings was chosen for conducting experiments. Three output responses in each experiment were normalized into a weighted grey relational grade using grey relational analysis coupled with the principal component analysis. The analysis of variance indicated that sliding distance is the most influential parameter followed by load and sliding velocity that contributes to the quality characteristics. Optimal results have been verified through additional experiments.*

Key Words: *Aluminum matrix composites, Taguchi method, Grey Relational Analysis, Principal component analysis, ANOVA*

1. INTRODUCTION

In the current world, there is an increase in demand for materials which have a high strength-to-weight ratio and greater wear and corrosion resistance. Hence, a lot of research has been dedicated to the development of advanced materials. One of the advanced materials is aluminum matrix composites (AMCs). They arouse interest, as they can be used in a wide range of applications, due to their low weight and high thermal resistance and conductivity. They are used particularly in the manufacturing of automotive components such as cylinder liners, pistons, drive shafts, brake rotors, cylinder heads, cylinder blocks, intake manifolds, rear axles and differential housings [1-3]. Shorowordi et al. [4] studied the dry sliding wear behavior of Al-13 wt% B_4Cp and Al-13 wt% SiC composites worn against a commercial

[a] Assistant Professor

phenolic brake pad under varying contact pressures at a constant sliding speed. The results show that the wear rate and friction coefficient of Al-B_4Cp composite are lower than those of Al-SiC MMC. Mahmoud et [5] investigated the dry-sliding wear performance of a hypereutectic A390 Al-Si alloy reinforced with graphite particulates (4% and 8%). They found that both the wear rate and coefficient of friction of the composites decreased considerably with the addition of graphite. Kaur et al. [6] preferred dry sliding wear for the effect of SiC reinforcement along with immiscible element in spray formed Al-Si base alloy. They found that Al-Si, Al-Si/SiC, Al-Si-5Sn/SiC & Al-Si-10SiC show that the nature of wear changes from lower loads to higher loads. The severe deformation wear occurs in spray formed alloy at higher loads. Poornesh Mangalorea et al [7] studied the tribological properties of Al 7079 alloy reinforced with agro waste particles. They found that the hardness and the tensile strength of the produced composite specimens are improved because of the synergic of the reinforcing particles and that the coconut shell ash is extremely helpful in reducing the wear rate. Alaneme et al [8] while studying about the corrosion and wear behavior of aluminum composites when reinforced with rice hush ash and alumina concluded that when aluminum alloy was reinforced with alumina alone, the resistance to corrosion was much higher than the resistance obtained after the addition of rice husk ash.

Apasi et al [9] investigated the wear behavior of aluminum alloy reinforced with coconut shell ash particles. They found out that, with the increase in the load, the wear rate of the composites also increased, since the contact friction between the pin and the disc increases. The addition of the ash reinforcement to the matrix was found to be useful since it helped in decreasing the wear rate. Shabani et al. [10] studied the effect of the reinforcement of SiC particles of varying size and volume fraction on the microstructure and tribological properties of Al-based composite. The hardness of material and applied normal load on pin have significant influence on tribological properties during dry sliding of Al6061/SiC composites. The mechanical properties and wear resistance of composites with a narrow size range of fly ash particles were superior to those of composites with a wide size range fly ash particles (Sudarshan et al. [11], [12]). Canakci et al. [13] prepared the CuSn10-graphite composite and investigated the microstructure, relative density, hardness, and abrasive wear behavior. They reported that the abrasive wear resistance increased with increasing graphite content and decreased with increasing sliding distance, applied load, and abrasive grit size. Modi et al. [14] showed the effect of the applied load on the wear rate of both zinc alloy and the 10 wt. % Al_2O_3 particle-reinforcement composite using statistical analyses of the measured wear rate at different operating conditions. The effect of the applied load on the wear rate of composite was found to be more severe. Considering the wear mechanisms, oxidative wear, delamination, two- or three-body abrasive wear and formation of a stable mechanically mixed layer (MML) are reported [15,16]. Mondal et al. [17] studied the influence of the applied load on the dry wear behavior of an Al–Zn–Mg alloy reinforced with SiC particles against a steel disc. By using the X-ray diffraction (XRD), they identified the presence of iron and aluminum oxides (Fe_2O_3 and Al_2O_3) together with intermetallic FeAl in the mechanically mixed layer.

Ezhil Vannan et al. [18] reported that the coefficient of thermal expansion of Al7075/basalt fiber metal matrix composites significantly decreases with the addition of basalt fiber. Bülent Öztürk et al. [19] studied the hot wear properties of ceramic and basalt fiber reinforced hybrid friction materials. Experiments showed that fiber content has a significant influence on the mechanical and tribological properties of the composites. The friction coefficient of the hybrid friction materials was increased with increasing additional basalt fiber content. But the specific wear rates of the composites decreased up to 30 vol% fiber content and then increased again above this value. Meenu et al. [20], attempted Taguchi grey relational

analysis to the experimental results in order to optimize the turning parameters for unidirectional GFRP composite and applied PCA to evaluate the weight corresponding to different performance characteristics. The principal component, having highest accountability proportion, was treated as single objective function for optimization (multi-response performance index). Therefore, in recent times the principal component analysis has been considered as an analytical tool for the optimization of a system with multiple performance characteristics [21-23]. Extensive researches on individual reinforcements of Titanium carbide and basalt improving the wear resistance and the strength of hybrid aluminum composites were carried out. However, very limited research was conducted in order to explore the combined effect of Titanium carbide and basalt particulate reinforcements on hybrid aluminum composites. Hence, in this study, an attempt has been made to investigate the wear behavior of the composite material under varying load, sliding speed and sliding distance and find the optimum parameter.

2. EXPERIMENTAL METHOD

Selection of materials and fabrication of composite

In this investigation, Al6061 was chosen as the base matrix. The percentage chemical composition of the Al6061 is given in Table 1. The reinforcement materials were Titanium carbide (TiC) and basalt powder. The hybrid metal matrix composite was prepared by adding 6% of TiC and 4% of basalt powder with Al6061.

Table1. Chemical Composition of Al6061

Mg	Si	Zn	Cu	Fe	Ti	Cr	Mn	Al
0.8-1.2	0.4-0.8	0.25	0.15-0.40	0.7	Max. 0.15	0.04-0.35	Max. 0.15	Remainder

The stir casting technique was employed to prepare the composite specimens. Al7075 was melted by raising its temperature to 850°C and degassed using a solid dry hexachloroethane compound. The titanium carbide and basalt powder particles were preheated for 30 min at 400°C for improving the wettability and added to the molten metal, and stirred continuously with an impeller at a speed of 600 rpm for 5 minutes. The melt with reinforcement particles was poured into a cylindrical permanent metallic mold and allowed to solidify. The die was released after 6 hours and the cast specimens were taken out.

Plan of experiment

Experiments have been conducted as per L9 orthogonal array for finding out the optimum test parameters. The main factors are the applied load (A), the sliding velocity (B), and the sliding distance (C). The levels of various control parameters are shown in Table 2.

Table 2. Process and Parameters and Levels

Level	Load (N)	Sliding Velocity (m/s)	Sliding Distance(m)
1	20	1.5	1000
2	30	2.3	1500
3	40	3.1	2000

The second column was assigned for the applied load (A), the third column for the sliding velocity (B), and the fourth column for the sliding distance (C). The response variables are the wear volume loss and the coefficient of friction of composites.

Experimental procedure

The dry sliding wear test of the specimens were conducted on a pin-on-disc (Fig. 1) wear testing machine (TR-20, DUCOM) according to ASTM G99-95 standards.

Fig. 1 Pin on disc apparatus

The cylindrical pin specimens having 10 mm diameter and 30 mm length machined out from the castings were used as test samples. Then, the ends of the specimens were polished metallographically.

The initial weight of the specimen was measured in the electronic weighing machine with the least count of 0.0001 g.

During the test, the pin was pressed against the counterpart rotating against the EN31 steel disc with the hardness of 65HRC by applying the load. After running through a fixed sliding distance, the specimens were removed, cleaned with acetone, dried and weighed to determine the weight loss due to the wear.

The results for various combinations of the parameters were obtained by conducting the experiment as an average of at least three runs as per the orthogonal array. It is presented in Table 3.

From the initial and final weight of the specimen, the initial and final volumes of the specimen are calculated using equations 1 and 2.

$$\text{Initial volume of the specimen} = \frac{\text{Initial weight of the specimen}}{\text{Density of the specimen}} \tag{1}$$

$$\text{Initial volume of the specimen} = \frac{\text{Initial weight of the specimen}}{\text{Density of the specimen}} \tag{2}$$

Then final volume loss of the specimen, the wear rate and the specific wear rate are calculated using eq. 3, 4, and 5 and are shown in table 3.

$$\text{Volume loss of the specimen} = \text{Final volume of the specimen- Initial volume of the specimen} \tag{3}$$

$$\text{Wear rate} = \frac{\text{Volume loss}}{\text{Sliding distance}} \quad \frac{\text{mm}^3}{\text{m}} \tag{4}$$

$$\text{Specific wear rate} = \frac{\text{Wear rate}}{\text{Load}} \quad \frac{\text{mm}^3}{\text{Nm}} \tag{5}$$

Table 3. Experimental plan and results

Expt no	Load (N)	Sliding Speed (m/s)	Sliding Distance (m)	Initial mass (g)	Final mass (g)	Wear rate (mm^3/m)	Friction force (N)	Specific wear rate (mm^3/Nm)
1	20	1.5	1000	6.854	6.84	0.005049	6.82	0.0002525
2	20	2.3	1500	6.148	6.131	0.004087	3.43	0.0002044
3	20	3.1	2000	6.598	6.58	0.003246	8.05	0.0001623
4	30	1.5	1500	6.00	5.98	0.004808	11.36	0.0001603
5	30	2.3	2000	6.59	6.57	0.003606	11.58	0.0001202
6	30	3.1	1000	6.96	6.94	0.007212	11.51	0.0002404
7	40	1.5	2000	6.61	6.58	0.005409	6.72	0.0001352
8	40	2.3	1000	6.59	6.53	0.021637	16.57	0.0005409
9	40	3.1	1500	6.53	6.512	0.004327	15.42	0.0001082

3. OPTIMIZATION STEPS

Signal-to-noise ratio

In Taguchi method, the signal-to-noise (S/N) ratio is used to represent a performance characteristic and the largest value of the S/N ratio is required. There are three types of S/Nratio -the lower-the-better, the higher-the-better, and the nominal-the-better. The S/N ratio with the lower-the-better characteristics (wear rate, coefficient of friction) can be calculated using eq. (6).

$$\eta_{ij} = -10\log\left(\frac{1}{n}\right)\sum_{j=1}^{n} y_{ij}^2 \tag{6}$$

where η_{ij} is the j^{th} S/N ratio of the i^{th} experiment, y_{ij} is the i^{th} experiment at the j^{th} test, *n* is the total number of tests.

The S/N ratio with a higher-the-better characteristic can be expressed as

$$\eta_{ij} = -10\log\left(\frac{1}{n}\right)\sum_{j=1}^{n} \frac{1}{y_{ij}^2} \tag{7}$$

The S/N ratio with a nominal-the-better characteristic can be expressed as

$$\eta_{ij} = -10\log\left(\frac{1}{ns}\sum_{j=1}^{n} y_{ij}^2\right) \tag{8}$$

where η_{ij} is the j^{th} S/N ratio of the i^{th} experiment, y_{ij} is the i^{th} experiment at the j^{th} test, n is the total number of tests, and s is the standard deviation.

Data pre-processing

In the GRA, the S/N ratio of quality characteristics is normalized first, to reduce the variability. Data preprocessing is a process of transferring the original sequence to a comparable sequence. For this purpose, the experimental results are normalized in the range 0 to 1. The normalization can be done from three different approaches.

In the present investigation, the main objective is to minimize the quality characteristics. Therefore, the lower-the-better criterion was selected for the normalization of experimental data, which is done by the following equation (eq. (9)):

$$X_i^*(k) = \frac{\max X_i^0(k) - X_i^0(k)}{\max X_i^0(k) - \min X_i^0(k)} \tag{9}$$

where $X_i^0(k)$ is the value after the grey relational generation (data preprocessing), max $X_i^0(k)$ is the largest value of $X_i^0(k)$, min$X_i^0(k)$ is the smallest value of $X_i^0(k)$, and X^0 is the desired value.

Grey relational coefficient and grey relational grade

After data pre-processing is carried out, the grey relational coefficient might be calculated to express the relationship between the ideal and actual normalized experimental results. The grey relational coefficient can be expressed as follows:

$$\xi_i(k) = \frac{\Delta_{\min} + \zeta\Delta_{\max}}{\Delta_{oi}(k) - +\zeta\Delta_{\max}} \tag{10}$$

where ζ(ϵ 0,1) = distinguished coefficient, ς=0.5 is generally used $\xi_i(k)$ is the grey relational coefficient, $\Delta_{\min}$ is the smallest value of Δ_{oi}(k), Δ_{max} is the largest value of Δ_{oi}(k) $\Delta_{oi}(k)$ is the deviation sequence of the reference sequence $X_o^*(k)$, and the comparability sequence $X_i^*(k)$, namely

$$\Delta_{oi}(k) = \|X_o(k) - X_i(k)\|$$

$$\Delta_{\max} = \max_{\forall j \in i} \max_{\forall k} \left\|X_o^*(k) - X_j^*(k)\right\|$$

$$\Delta_{\min} = \min_{\forall j \in i} \min_{\forall k} \left\|X_o^*(k) - X_j^*(k)\right\|$$

Finally, the grey relational grade (GRG) in each experiment is evaluated through its corresponding average-GRCs as given in eq. 11.

GRG is for showing the correlation among the experimental data.The higher the GRG, the better the experimental plan.

$$\gamma_i = \frac{1}{n}\sum_{k=1}^{n} w_n \xi_i(k) \text{ where } \sum_{k=1}^{n} w_n = 1 \tag{11}$$

where γ_i is the weighted grey relational grade for the ith experiment and n is the number of performance.

In this study, PCA was used to obtain the w_n.

Through the linear combinations among the responses, the PCA explores the structure of the variance-covariance.

The procedure of PCA is explained in the following section.

Principal component analysis (PCA)

Principal Component Analysis (PCA) was proposed by Pearson [24], and developed as a statistical tool by Hotelling [25].

Initially, this technique has been applied to quantify and identify phenomena in social sciences where it was difficult to directly measure the phenomenal changes.

PCA is useful in reduction of data and interpretation of multi-objective sets of data. Currently, PCA is finding wide applications in various scientific fields. The procedure is described as follows.

1. The original multiple performance characteristic array

$$X = \begin{bmatrix} x_1(1) & x_1(2) & \ldots\ldots & \ldots\ldots & x_1(n) \\ x_2(1) & x_2(2) & \ldots\ldots & \ldots\ldots & x_2(n) \\ . & . & \ldots\ldots & \ldots\ldots & . \\ . & . & \ldots\ldots & \ldots\ldots & . \\ x_m(1) & x_m(2) & \ldots\ldots & \ldots\ldots & x_m(n) \end{bmatrix}, \qquad x_i(j), i = 1,2,\ldots\ldots\ldots m;\ \ j = 1,2,\ldots\ldots\ldots n \tag{12}$$

where m is the number of experiment and n is the number of the performance characteristic.

In this paper, X is the grey relational coefficient of each performance characteristic and m=9 and n=3.

2. Correlation coefficient array

The correlation coefficient array is evaluated as follows:

$$R_{jl} = \left(\frac{Cov(x_i(j), x_i(l))}{\sigma_{x_i}(j) \times \sigma_{x_i}(l)}\right), \qquad j = 1,2,3 \ldots\ldots n, \qquad l = 1,2,3 \ldots\ldots . n \tag{13}$$

where $Cov(x_i(j), x_i(l))$ is the covariance of sequences $x_i(j)$ and $x_i(l)$, $\sigma_{xi}(j)$ is the standard deviation of sequence $x_i(j)$ and $\sigma_{xi}(l)$ is the standard deviation of sequence $x_i(l)$.

3. Determining the eigenvalues and eigenvectors

The Eigenvalues and Eigenvectors are determined from the correlation coefficient array,

$$(R\text{-}\lambda_k I_m)V_{ik} = 0 \tag{14}$$

where λ_k = Eigen values, $\sum_{k=1}^{n} \lambda_k = n$, k=1,2……n; V_{ik}= $[a_{k1}\ ak\ a_{k2}\ \ldots.\ a_{kn}]^T$ Eigen vectors corresponding to the Eigen value λ_k.

4. Principal components

The principal component is formulated as:

$$Y_{mk} = \sum_{i=1}^{n} X_m(i).V_{ik} \tag{15}$$

where Y_{m1} is called the first principal component, Y_{m2} is called the second principal component, and so on.

The principal components are aligned in descending order with respect to variance, and therefore, the first principal component Y_{m1} accounts for most variance in the data.

Analysis and discussion of experimental results

In this study, wear rate, the friction force and the specific wear rate of TiC and basalt based aluminum MMC for different combination of wear parameters of nine experimental runs are considered. The following sequential steps are adopted to determine the optimal combinations of the wear parameters based on grey relational analysis coupled with principal component analysis:

1. The S/N ratios for the experimental data were calculated.
2. The S/N ratios were normalized.
3. The corresponding grey relational coefficients were calculated.
4. PCA was used and the grey relational grades were calculated.
5. The optimal levels of wear parameters were obtained.
6. Finally, the confirmation experiments were conducted.

As per the optimization procedure, the S/N and normalized S/N ratios for the wear rate, the friction force and the specific wear rate were calculated and the results are tabulated in Table 4.

Table 4. S/N ratio values and normalized S/N ratio values

Ex no	S/N ratio			Normalized S/N ratio		
	Wear rate (mm^3/m)	Friction Force (N)	Specific wear rate (mm^3/Nm)	Wear rate (mm^3/m)	Friction Force (N)	Specific wear rate (mm^3/Nm)
1	45.93589259	-16.675687	71.9564925	0.232879	0.436371	0.52652808
2	47.77190725	-10.705882	73.7925072	0.12145	0	0.39519846
3	49.77302969	-18.115917	75.7936296	0	0.541647	0.25205874
4	46.36071082	-21.107566	75.9031359	0.207096	0.760325	0.24422578
5	48.85948555	-21.274171	78.4019107	0.055444	0.772504	0.06548913
6	42.83888564	-21.221506	72.3813107	0.420839	0.768654	0.49614095
7	45.33766037	-16.547385	77.3788602	0.269186	0.426993	0.13866764
8	33.29605910	-24.386450	65.3372589	1	1	1
9	47.27626210	-23.761687	79.3174619	0.151531	0.954332	0

Table 5. Gray relational co-efficient

Ex. no	Grey relational coefficient		
	Wear rate	Friction Force	Specific wear rate
1	0.682241	0.533976	0.48707874
2	0.80457	1	0.55853536
3	1	0.480009	0.66484169
4	0.707117	0.396723	0.67183913
5	0.900181	0.392926	0.8841903
6	0.542983	0.394118	0.501937
7	0.650038	0.539379	0.78287981
8	0.333333	0.333333	0.33333333
9	0.767423	0.3438	1

PCA was adopted to determine the corresponding weighting values for each performance characteristic to reflect its relative importance in the grey relational analysis. The elements of

the array for multiple performance characteristics listed in Table 5 represent the grey relational coefficient of each performance characteristic. These data were used to evaluate the correlation coefficient matrix and to determine the corresponding Eigenvalues from Eq. (14). The Eigenvalues are shown in Table 6.

Table 6. The eigenvalues and explained variation for principal components

Principal components	Eigenvalues	Explained variation (%)
First	1.0682	35.61
Second	0.9460	31.53
Third	0.9858	32.86

The Eigenvector corresponding to each Eigenvalue is listed in Table 7. The square of the Eigenvalue matrix represents the contribution of the respective performance characteristic to the principal component. The contribution of the wear rate, the friction force and the specific wear rate is shown in Table 8.

Table 7. The eigenvectors for principal components

Performance characteristics	First principal component	Second principal Component	Third principal component
Wear rate	-0.6361	-0.6937	0.3379
Friction force	-0.4176	-0.0587	-0.9067
Specific wear rate	-0.6489	0.7179	0.2523

Table 8. The most variance contribution of each individual performance characteristic for the principal component

Performance characteristics	Contribution/weighted value
Wear rate	0.405
Friction force	0.174
Specific wear rate	0.421

The contributions of each individual performance characteristic for the principal component are 0.405, 0.174 and 0.421. Moreover, the variance contribution for the first principal component characterizing the three performance characteristics is as high as 35.61%. Hence, for this study, the squares of its corresponding Eigenvectors were selected as the weighting values of the related performance characteristic, and coefficients w1, w2, and w3 in Eq. 11 were thereby set as 0.405, 0.174 and 0.421, respectively. Based on Eq. 11 and data listed in Table 6, the grey relational grades were calculated and shown in Table 9.

Table 9. Grey relation grades (GRG's) and its rank

Ex no	Grey relation grades (GRG)	Rank
1	0.19142655	7
2	0.24499813	4
3	0.25613998	3
4	0.21275219	6
5	0.26839556	1
6	0.16660012	8
7	0.2289032	5
8	0.11111111	9
9	0.26387593	2

Thus, the optimization design was performed with respect to a single grey relational grade rather than complicated performance characteristics. According to performed experimental design, it is clearly observed from Table 9 that the wear parameters setting of experiment no. 5 has the highest grey relational grade.

Thus, the fifth experiment gives the best multi-performance characteristics among the nine experiments.

From the value of grey relational grade in Table 9, the main effects are tabulated in Table 10 and the factor effects are plotted in Fig. 2.

From table 9 and Fig. 2, the optimum factors for both the wear rate and the coefficient of friction obtained for the hybrid composite are 20 N load (level 1), 3.1 m/s sliding speed (level 3), and 2000 m sliding distance (level 3) combination.

Table 10. Main effects on grey grades

Level	Load	Sliding velocity	Sliding distance
1	0.2309*	0.2110	0.1564
2	0.2159	0.2082	0.2405
3	0.2013	0.2289*	0.2511*
Delta	0.0296	0.0207	0.0948
Rank	2	3	1

*Optimum level

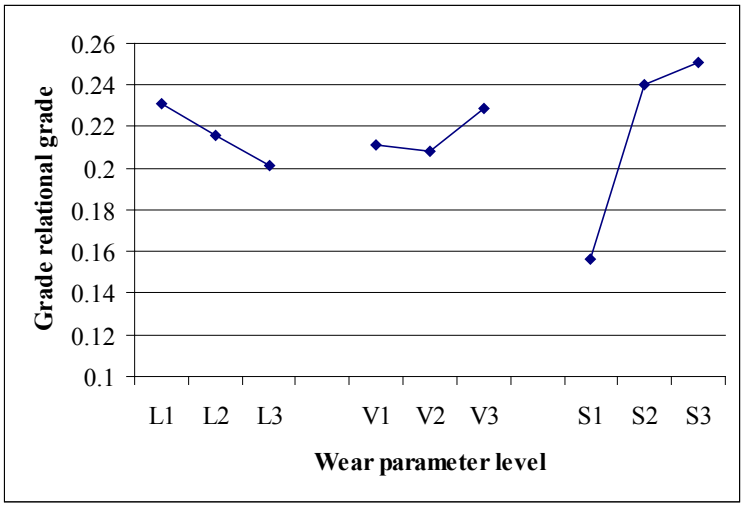

Fig. 2 Effect of wear parameter levels on the multi-performance

Analysis of variance

The purpose of the analysis of variance (ANOVA) is to find which wear parameters significantly affect the performance characteristic. This is accomplished by separating the total variability of the grey relational grades, which is measured by the sum of the squared deviations from the total mean of the grey relational grade, into contributions by each wear parameters and the error.

This analysis was carried out for a level of significance of 5%, i: e., the level of confidence 95%. Results of ANOVA (Table 11) for the GRG, indicate that the sliding distance (74.504%) influences more on the multi-performance characteristics of Al6061/TiC/basalt hybrid composite followed by load (6.038 %) and sliding velocity (3.477%).

Table 11. Results of ANOVA for GRG

Source	DF	Adj SS	Adj MS	F	P	%C
Load	2	0.001311	0.000655	0.38	0.726	6.038
Sliding velocity	2	0.000755	0.000378	0.22	0.821	3.477
Sliding distance	2	0.016177	.008088	4.66	0.177	74.504
Residual Error	2	0.003470	0.001735			15.981
Total	8	0.021712				100

Confirmation Experiments and Coclusions

After the optimal level of parameters is identified, a confirmation experiment is carried out to predict and verify the improvement of the quality characteristic using the optimal level of the design parameters. The predicted grey relational grades of using the optimum level of the dry sliding parameters are calculated using Eq. 16.

$$\hat{\gamma} = \gamma_m + \sum_{i=1}^{q} (\overline{\gamma_i} - \gamma_m) \tag{16}$$

where γ_m is the total mean grey relational grade, $\overline{\gamma_i}$ is the mean grey relational grade at the optimum level, and 'q' is the number of main parameters that significantly affect the coefficient of friction and wear rate. Table 12 shows the comparison of the predicted grey relational grade with the actual grey relational grade obtained in the experiment using the optimal process parameters.

Table 12. Results of confirmation experiments

	Initial testing parameters	Optimum testing parameters	
		Prediction	Experiment
Combination of testing parameters	A1B1C1	A1B3C3	A1B3C3
Wear rate	0.005049		0.003606
Friction force	6.82		11.58
Specific wear rate	0.0002525		0.0001202
Grey relational grade	0.19142655	0.278828083	0.26839556

From Table 12, it is clear that the optimal data obtained from the confirmation test, which was conducted with the level settings parameters of load (20 N) (level 1), sliding velocity (3.1 m/s) (level 3) and sliding distance (2000 m) (level 3) had good agreement with the predicted model. Hence, the grey relational analysis based on Taguchi method for the optimization of the multi response problems is a very useful tool for predicting the wear rate and the coefficients wing conclusions were drawn:

- The Al6061/Titanium carbide/ Basalt hybrid composites have been successfully produced by the stir casting route.
- The principal component analysis (PCA) based grey relational analysis (GRA) for the optimization of the multi-response problems is a very useful tool for predicting the wear rate, the friction force and the specific wear rate of Al6061/Titanium carbide/ Basalt hybrid Metal Matrix Composites.
- From, ANOVA, it is revealed that the sliding distance (74.504%) influences more on the multi-performance characteristics of hybrid composite followed by load (6.038%) and sliding velocity (3.477%).

REFERENCES

[1] W. S. Miller, L. Zhuang, J. Bottema, A. J. Wittebrood, P. D. Smet, A. Haszler, A. Vieregge, Recent development in aluminium alloys for the automotive industry, *Materials Science & Engineering A,* **280,** 37–49, 2000.

[2] I. Sinclair, P. J. Gregson, Structural performance of discontinuous metal matrix composites, *Materials Science and Technology*, **13**, 709–726, 1997.

[3] A. Ibrahim, F. A. Mohamed, E. J. Lavernia, Particulate Reinforced Metal Matrix Composites – A Review, *Journal of Materials Science*, **24**, 1137–1156, 1991.

[4] K. M. Shorowordi, A. Haseeb, J. P. Celis, Tribo-surface characteristics of Al–B4C and Al–SiC composites worn under different contact pressures, *Wear*, **261**, 5-6, 634-641, 2006.

[5] T. S. Mahmoud, Tribological behaviour of A390/GrP metal-matrix composites fabricated using a combination of rheocasting and squeeze casting techniques*, Journal of Mech. Engin. Science*, **222,** 257–265, 2008.

[6] K. Kaur, R. Anant, O. P. Pandey, Tribological Behaviour of SiC Particle Reinforced Al-Si Alloy, *Tribology Letters*, **44**, 41-58, 2011.

[7] P. Mangalore, C. S. Vittal, Akash, A. Ulvekar, Abhiram, J. Sanjay, Advaith, *Study of tribological properties of Al 7079 alloy reinforced with agro waste particles*, AIP Conference Proceedings, 2019.

[8] K. K. Alaneme, P. A. Olubambi, Corrosion and wear behaviour of rice husk ash—Alumina reinforced Al–Mg–Si alloy matrix hybrid composites, *Journal Material Research Technology*, **2**, 188–194, 2013.

[9] A. Apasi, P. B. Madakson, D. S. Yawas, V. S. Aigbodion. Wear Behaviour of Al-Si-Fe Alloy/Coconut Shell Ash Particulate Composites, *Tribology in Industry*, **34**, 36-43, 2012.

[10] A. Mazahery, M. O. Shabani, Microstructural and abrasive wear properties of SiC reinforced aluminum-based composite produced by compocasting, *Transac. of Nonfer. Metals Society of China,* **23**, 1905–1914, 2013.

[11] Sudarshan, M. K. Surappa, Dry Sliding Wear of Fly Ash Particle Reinforced A356 Al Composites, *Wear*, **265,** 349–360, 2008.

[12] Sudarshan, M. K. Surappa, Synthesis of Fly Ash Particle Reinforced A356 Al Composites and Their Characterization, *Materials Science and Engineering A*, **480**, 117–124, 2008.

[13[A. Canakci, H. Cuvalci, T. Varol, Microstructure and abrasive wear behavior of CuSn10-Graphite composites produced by powder metallurgy, *Powder Metallurgy and Metal Ceramic,* **53**(5-6), 275-287,2014.

[14] O. P. Modi, R. P. Yadav, D. P. Mondal, R. Dasgupta, S. Das, A. H. Yagnesaran, Abrasive wear of Zinc-Al alloy-10% Al_2O_3 composite through factorial design, *Journal of Material Science* **36**, 1601-1607, 2001.

[15] F. Gul, M. Acilar, Effect of the reinforcement volume fraction on the dry sliding wear behavior of Al-10Si/SiCp composites produced by vacuum infiltration technique, *Composite Science and Technology,* **64**, 1959–1970, 2004.

[16] M. Acilar, F. Gul, Effect of the applied load, sliding distance and oxidation on the wear behavior of Al-10Si/SiCp composites produced by vacuum infiltration technique, *Materials and Design,* **25**, 209–217, 2004.

[17] D. P. Mondal, S. Das, R. N. Rao, M. Singh, Effect of SiC addition and running-in wear on the sliding wear behaviour of Al–Zn–Mg aluminium alloy, *Materials Science and Engineering,* **402**, 307–319, 2005.

[18] S. Ezhil Vannan, S. Paul Vizhian, R. Karthigeyan, Investigation on the influence of basalt fiber on thermal properties of Al7075/basalt fiber metal matrix composites, *Procedia Engineering*, **97**,432–438, 2014.

[19] B. Öztürk, F. Arslan and S. Öztürk, Hot wear properties of ceramic and basalt fiber reinforced hybrid friction materials, *Tribology International*, **40**, 37-48, 2007.

[20] M. Gupta, S. Kumar, Investigation of surface roughness and MRR for turning of UD-GFRP using PCA and Taguchi method, *Engin. Science and Technology*, *An International Journal,* **18**(1), 70-81, 2015.

[21] T. Fu, J. Zhao, W. Liu, Multi-objective optimization of cutting parameters in high-speed milling based on grey relational analysis coupled with principal component analysis, *Frontiers of Mechanical Engineering*, **7**(4), 445-452, 2012.

[22] A. P. Paiva, S. C. Costa, E. J. Paiva, P. P. Balestrassi, J. R. Ferreira, Multi-objective optimization of pulsed gas metal arc welding process based on weighted principal component scores, *The International Journal of Advanced Manufacturing Technology*, **50**(1-4), 113-125, 2010.

[23] D. M. D. Costa, T. I. Paula, P. A. P. Silva, A. P. Paiva, Normal boundary intersection method based on principal components and Taguchi's signal-to-noise ratio applied to the multiobjective optimization of 12L14 free machining steel turning process, *The International Journal of Advanced Manufacturing Technology*, **87**, 825-834, 2016.

[24] K. Pearson, On lines and planes of closest fit to systems of points in space, *Philos Mag* **62**:559–572, 1901.

[25] H. Hotelling, Analysis of a complex of statistical variables into principal components, *Journal of Educational Psychology,* **24**(6), 417–441, 1993.